



# Comparative Analysis of Concurrent vs Sequential Administration of anti-PD-I Following Thoracic Radiotherapy: Impact on Lung Tissue Damage

Dose-Response:  
An International Journal  
January-March 2025:1-9  
© The Author(s) 2025  
Article reuse guidelines:  
[sagepub.com/journals-permissions](https://sagepub.com/journals-permissions)  
DOI: 10.1177/15593258251322324  
[journals.sagepub.com/home/dos](https://journals.sagepub.com/home/dos)  


Peng Yan<sup>1</sup> , Zewen Wang<sup>1</sup>, Yufeng Wang<sup>1</sup>, Yongliang Liu<sup>1</sup>, Anna Tong<sup>2</sup>, and Meili Sun<sup>1</sup>

## Abstract

The combination of thoracic radiotherapy and immune checkpoint inhibitors (ICIs) had demonstrated a synergistic therapeutic effect, albeit with the occurrence of overlapping pulmonary toxicities. We established a mouse model using programmed cell death protein-1 (PD-1) antibody at different time points after thoracic radiotherapy. Hematoxylin and eosin (HE) staining, as well as TUNEL staining, were utilized for the morphological assessment of lung tissue damage. Inflammatory cells and cytokines present in bronchoalveolar lavage fluid (BALF) were analyzed using flow cytometry and cytometric bead array immunoassay (CBA). Additionally, immunohistochemistry (IHC) and immunofluorescence (IF) staining were conducted to observe the infiltration of inflammatory cells in lung tissue. Immediate administration of PD-1 antibody after thoracic radiotherapy resulted in more severe lung tissue injury compared to delayed administration. Concurrent treatment led to an increase in lymphocytes and neutrophils in BALF, as well as higher levels of inflammatory cytokines. IHC and IF analysis revealed that neutrophils, macrophages, and lymphocytes were more prominent in the concurrent treatment group. A more severe lung injury occurred when PD-1 antibody was given simultaneously with thoracic radiotherapy, possibly due to increased inflammation caused by the combination treatment.

## Keywords

thoracic radiotherapy, ICIs, PD-1, pneumonitis, timing sequence

## Introduction

Radiotherapy had been used as a radical or palliative treatment option for thoracic cancers.<sup>1-4</sup> Thoracic radiotherapy combined with immune checkpoint inhibitors (ICIs) had gained popularity in recent years, and numerous studies had reported on the synergistic benefits of combining radiotherapy with ICIs.<sup>5,6</sup>

Although combination therapy had advantages, potential toxicity must be taken into account. Radiation pneumonitis had been estimated to occur in 10%-30% of patients treated with radiotherapy for thoracic malignancies,<sup>7</sup> while the incidence of ICIs-associated pneumonitis was estimated to be range between 3% and 6%.<sup>8</sup> The combination therapy had raised concerns regarding potential pulmonary toxicity. In the secondary analysis of the KEYNOTE-001 trial, all-grade

pneumonitis occurred more frequently in patients who had received previous thoracic radiotherapy compared to those with no previous thoracic radiotherapy (63% vs 40%).<sup>9</sup> In the PEMBRO-RT trial, pneumonitis occurred more often in the

<sup>1</sup> Department of Oncology, Jinan Central Hospital, Shandong First Medical University, Jinan, China

<sup>2</sup> Department of Radiation Oncology, 960 Hospital of the PLA Joint Logistics Support Force, Jinan, China

Received 1 July 2024; accepted 24 January 2025

## Corresponding Author:

Meili Sun, Department of Oncology, Jinan Central Hospital, Shandong First Medical University, No 105 Jiefang Road, Jinan 250013, China.  
Email: [smlil980@163.com](mailto:smlil980@163.com)



Creative Commons Non Commercial CC BY-NC: This article is distributed under the terms of the Creative Commons Attribution-NonCommercial 4.0 License (<https://creativecommons.org/licenses/by-nc/4.0/>) which permits non-commercial use, reproduction and distribution of the work without further permission provided the original work is attributed as specified on the SAGE

and Open Access pages (<https://us.sagepub.com/en-us/nam/open-access-at-sage>).

pembrolizumab combined with radiotherapy group than in the control group (26% vs 8%).<sup>10</sup>

The timing of combination therapy might impact the incidence of adverse events (AEs). For instance, in a study, the incidence of AEs was 39% when ICIs were administered within 14 days of thoracic radiotherapy, which decreased to 23% when the interval exceeded 14 days.<sup>11</sup> European Society for Medical Oncology (ESMO) 2020 congress suggested that the application of PD-1 blockade before or during thoracic radiotherapy increased the incidence of radiation pneumonitis compared to administration after radiotherapy (60% vs 28%,  $P = .01$ ).<sup>12</sup>

Enhanced comprehension of pulmonary toxicity could improve strategies for prevention and management in combined therapeutic approaches. An animal model was developed to investigate the impact and initial underlying mechanisms.

## Methods

### *Establishment of Acute Radiation Lung Injury Mice Model*

Male C57BL/6 mice (6-8 weeks old, 18-22 g) were purchased from the SiPeiFu Biotechnology Co., Ltd., Beijing, China. Mice were housed under standard laboratory conditions, and sterilized food and water were supplied. Animal welfare was in accordance with Institutional and Office of Laboratory Animal Welfare Guidelines. We intravenously injected  $1 \times 10^5$  Lewis lung cancer (LLC) cells into the mice via the tail vein to establish the lung metastasis model. After 2 weeks, the acute radiation pneumonitis model was established based on previous studies.<sup>13</sup> Mice were anesthetized and exposed to whole thorax radiation with X-rays at a dose rate of 600.00 cGy/min and a cumulative radiation dose of 18 Gy delivered by a linear accelerator (Elekta, Stockholm, Sweden) at Jinan Central Hospital, Shandong First Medical University. The animal experiments were approved by the Ethical Committee of Central Hospital Affiliated to Shandong First Medical University at August 2021 (NO JNCHIAUCUC2021-26).

### *PD-1 Blockade Was Administered at Different Intervals After Irradiation*

Anti-PD-1/PD-L1 therapy represented the predominant class of ICIs employed in the treatment of advanced non-small cell lung cancer (NSCLC) lacking driver mutations.<sup>14</sup> Consequently, the anti-PD-1 antibody (Bio X Cell, West Lebanon, NH) was selected for subsequent experimentation. Ten mice were randomly assigned to 2 groups after irradiation, with each group comprising 5 mice. One group receiving concurrent administration of anti-PD-1 antibody following irradiation, while the other group receiving sequential administration of anti-PD-1 antibody following irradiation. The administration protocol for the anti-PD-1 antibody was

based on previous research.<sup>15</sup> Figure 1 illustrated 2 distinct dosing approaches: concurrent dosing, which involved intraperitoneal injection of the anti-PD-1 antibody (200  $\mu\text{g}/\text{mouse}$ ) on days 1, 3, and 5 following irradiation, and sequential dosing, which entailed intraperitoneal injection on days 14, 16, and 18 after irradiation.

### *Mice Sacrificed and Sample Collection*

All mice were sacrificed on the 28th day after irradiation. The removed lungs were lavaged and pooled 3 times with 1 mL of ice-cold PBS. The obtained bronchoalveolar lavage fluid (BALF) was centrifuged at  $3000 \times g$  for 10 min at  $4^\circ\text{C}$ , the sediment was used for flow cytometry and the supernatants were used for cytokine detection. The lungs were then immersed in 4% paraformaldehyde for 48 h and embedded in paraffin.

### *Histological Analysis, Immunohistochemistry (IHC) and Immunofluorescence (IF)*

Histopathological changes were determined by hematoxylin eosin (HE) staining. Alveolar congestion, hemorrhage, aggregation of inflammatory cells in airspaces or vessel walls and the thickness of the alveolar walls were assessed by 0-4 point semi-quantitative histological analysis (4: Extremely serious, 3: Serious, 2: Middle, 1: Slight, 0: Normal). Each of these 4 parameters was assessed using a severity scale ranging from 0 to 4. The average score was calculated by summing the individual scores and subsequently dividing the total by 4.<sup>16</sup>

IHC was performed as previously described.<sup>17</sup> The primary antibodies used in our study were listed below: Myeloperoxidase (MPO) (Boster, cat. no. BA0544, 1:300), F4/80 (CST, cat. no. 70076, 1:300). Immunohistochemical analysis was performed by 2 independent pathologists. The proportion score represented the estimated fraction of positive staining cells (0 = none; 1 = less than 25%; 2 = 25%-75%; 3 = greater than 75%). The intensity score represented the average staining intensity of positive cells (0 = none; 1 = weak; 2 = intermediate; 3 = strong). The 2 scores were multiplied to generate the immunoreactivity score (IS) for each case (range = 0-9).

IF was carried out as described previously.<sup>18</sup> Lung tissues embedded in paraffin were sliced into 5  $\mu\text{m}$  sections, permeabilized, and treated with a blocking solution containing 5% donkey serum. Subsequently, the sections were incubated with antibodies targeting CD4 (Invitrogen cat. no. 14-9766-82) and CD8 (CST cat. no. 98941). Finally, fluorescently labeled secondary antibody and DAPI staining solution were added. Images were captured using a fluorescence microscope (Model BX-53, Olympus). The fluorescence intensity was measured with ImageJ software. For quantitative analysis of IHC/IF, each slice was randomly photographed from 5 different fields.

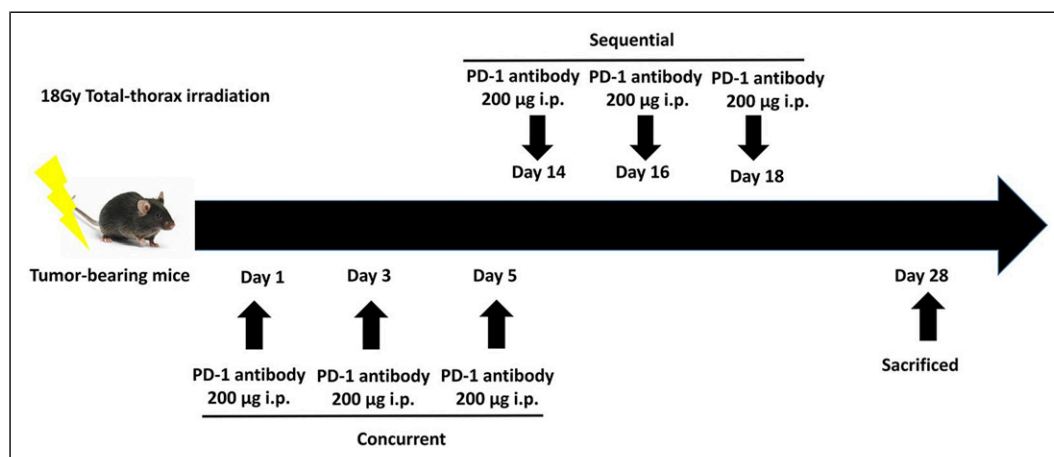


**Figure 1.** Administration paradigms of anti-PD-1 antibody in thoracic irradiation mice model. Concurrent: after the initial 18 Gy thoracic irradiation, mice were intraperitoneally injected with anti-PD-1 antibody (200 µg per mouse each time) on days 1, 3 and 5. Sequential: After the initial 18 Gy thoracic irradiation, mice were intraperitoneally injected with anti-PD-1 antibody (200 µg per mouse each time) on days 14, 16 and 18.

### TUNEL Assay

As for TUNEL staining, the rehydrated tissue slice was stained using a TUNEL staining kit (Beyotime) according to the manufacturer's protocol. The number of the TUNEL-positive cells in 5 fields ( $\times 100$ ) was counted, averaged as the number of cells per field.

### Flow Cytometry Detection of BALF After Collection

The collected BALF cells were stained 30 min at 4°C in 0.2% bovine serum albumin in PBS containing 1:100 dilution of the following antibodies: APC-Cy7 anti-mouse CD45 (BD Biosciences, cat. no. 557659), APC anti-mouse CD3 (CST, cat. no. 24265), FITC anti-mouse CD4 (CST, cat. no. 96127), BV605 anti-mouse CD8 (BD Biosciences, cat. no. 563152), PE anti-mouse CD11b (CST, cat. no. 24965), BV421 anti-mouse F4/80 (BD Biosciences, cat. no. 565411), PerCP-cy5.5 anti-mouse ly6G (CST, cat. no. 63460). BD Canto II flow cytometer was used for analytical cell counts, analysis was performed with Diva software (FACS Diva, 8.02).

### Cytokines From the BALF Were Analyzed With Cytometric Bead Array (CBA) Immunoassay

CBA Mouse Inflammation Kit were purchased from BD Biosciences (cat. no. 552364, Franklin Lakes, NJ, USA). The particles were bound by a covalent bond to an antibody against one of the cytokines: interferon- $\gamma$  (IFN- $\gamma$ ), monocyte chemoattractant protein-1 (MCP-1), interleukin-6 (IL-6), IL-10, IL-12 and tumor necrosis factor (TNF). 50 µL of the sample or cytokine standard was added to the mixture of 50 µL of each of antibody-PE detector and antibody-bead reagent. The mixture was incubated for 160 min in the dark at room temperature and washed, and the test samples

were acquired using the flow cytometer (BD FACS Canto II).

### Statistical Analysis

Statistical analysis was performed by SPSS 23.0 software and Prism Graphpad 8.0. Student's *t*-test was used to test differences. All data shown were expressed as the mean  $\pm$  Standard Deviation (SD). All tests were two-tailed, and  $P < .05$  was considered statistically significant.

## Results

### The Effect of the Sequence of Combination Therapy on Lung Injury

HE staining and TUNEL staining were utilized to assess injury in the lung tissue sections (Figure 2). Evaluation of lung injury through HE staining included assessment of alveolar congestion, hemorrhage, aggregation of inflammatory cells in airspaces, and thickness of alveolar walls. The severity of lung tissue injury was found to be significantly greater in the concurrent treatment group compared to the sequential treatment group, with scores of  $3.10 \pm .29$  and  $2.30 \pm .20$ , respectively ( $P = .001$ ).

The TUNEL assay was conducted to detect apoptotic cells, with the concurrent treatment group exhibiting a higher number of apoptotic cells per field ( $370.3 \pm 50.5$ ) compared to the sequential treatment group ( $255.5 \pm 33.2$ ),  $P = .003$ .

### Effect of Therapy Sequence on Inflammatory Cell Subsets in BALF

We detected inflammatory cells including total lymphocytes, CD4<sup>+</sup> T lymphocytes (CD3<sup>+</sup>CD4<sup>+</sup>), CD8<sup>+</sup>T

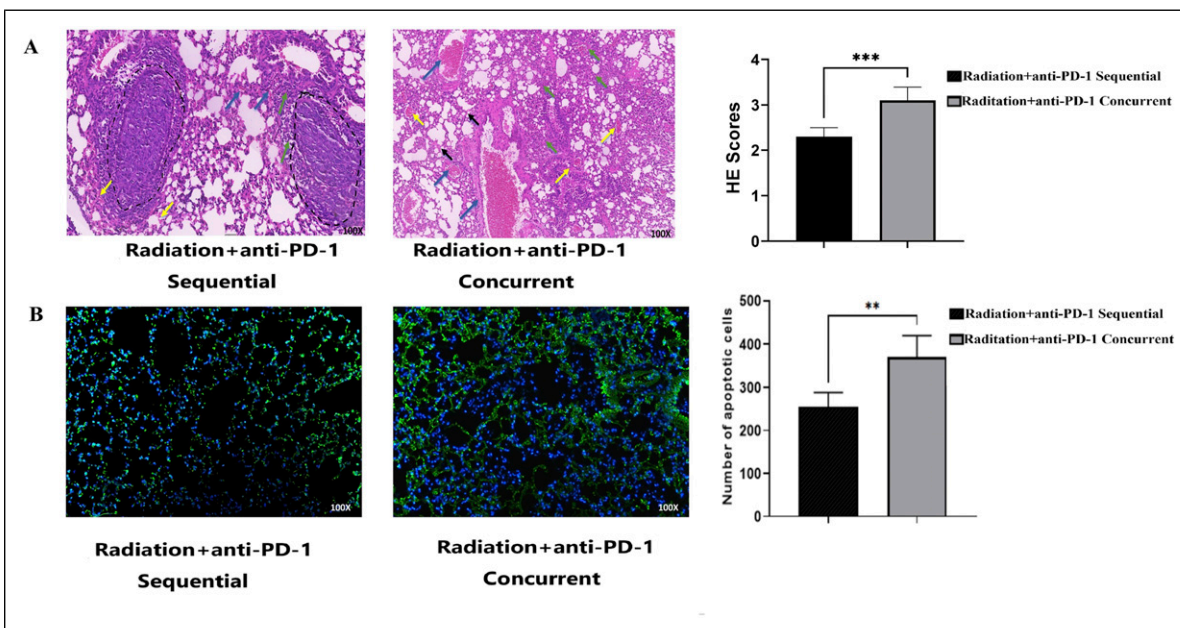


**Figure 2.** Evaluate lung tissue morphology in different treatment sequences using HE and TUNEL staining. (A) Representative HE staining images of lung tissue. The blue arrow shows alveolar congestion, the yellow indicates hemorrhage, the black marks thickened alveolar walls, and the green highlights inflammatory cell aggregation in airspaces or vessel walls. The dotted line delineates the boundary of tumors located within the lung. On the right is a statistical graph of inflammatory scores. (B) Representative TUNEL staining images of lung tissue. Displayed on the right is a statistical diagram illustrating apoptotic cells. \* $P < .05$ , \*\* $P < .01$ , \*\*\* $P < .001$ .

lymphocytes ( $CD3^+CD8^+$ ), neutrophils ( $Ly6G^+CD11b^+F4/80^-$ ), and macrophages ( $CD11b^+F4/80^+$ ) by flow cytometry. As shown in Figure 3, the results indicated a significant increase in the proportions of lymphocytes and neutrophils in BALF in the concurrent treatment group, which exhibited values of  $41.26\% \pm 3.30\%$  and  $7.34\% \pm .68\%$ , respectively. In contrast, the sequential treatment group demonstrated lower proportions of lymphocytes and neutrophils, recorded at  $17.82\% \pm 1.97\%$  and  $2.88\% \pm .53\%$ , respectively. Both comparisons yielded  $P$  values of less than .0001. The proportion of macrophages in the BALF was significantly decreased in the concurrent treatment group compared to the sequential treatment group, with proportions of  $38.92\% \pm 4.54\%$  and  $67.26\% \pm 3.33\%$ , respectively ( $P < .0001$ ).

T cell subpopulation analysis showed that the proportion of  $CD4^+$ T cells in the concurrent treatment group was  $46.22\% \pm 3.47\%$ , significantly higher than that in the sequential treatment group ( $39.08\% \pm 2.65\%$ ) ( $P = .0064$ ).

#### Effect of Therapy Sequence on Inflammatory Cytokines in BALF

Six cytokines, IL-6, IL-10, MCP-1, IFN- $\gamma$ , IL-12 and TNF were detected in the BALF (Figure 4). Compared with the sequential treatment group, IL-6, IL-10, MCP-1 and TNF in the concurrent treatment group were significantly increased in BALF ( $P < .01$ ).

#### Effect of Combination Therapy Sequence on Inflammatory Cells Infiltration in Lung Tissue

CD4 and CD8 were employed for the quantification of lymphocyte populations, MPO was utilized for the detection of neutrophils, and F4/80 served as a macrophage-specific marker for the identification of macrophages (as shown in Figure 5). Neutrophil infiltration, macrophage infiltration and lymphocyte infiltration in the concurrent treatment group were significantly increased. There was a significant increase in  $CD4^+$ T cells in the concurrent treatment group, whereas  $CD8^+$ T cells did not exhibit a significant increase.

#### Discussion

Recently, when thoracic radiotherapy was combined with ICIs, there were typically 2 approaches. One approach involved a concurrent treatment model, exemplified by the ETOP NICOLAS phase II trial, which evaluated the safety and efficacy of nivolumab (PD-1) in combination with chemoradiotherapy for stage III NSCLC.<sup>19</sup> Similarly, the KEYNOTE-799 study administered thoracic radiotherapy, pembrolizumab (PD-1), and platinum-based chemotherapy concurrently to patients.<sup>20</sup> Alternatively, a sequential approach was employed, as demonstrated in the PACIFIC study, where thoracic irradiation was followed by durvalumab (PD-L1). In this study, durvalumab was used as maintenance therapy 1-42 days after the completion of concurrent chemoradiotherapy.<sup>21</sup> The Hoosier Cancer Research Network

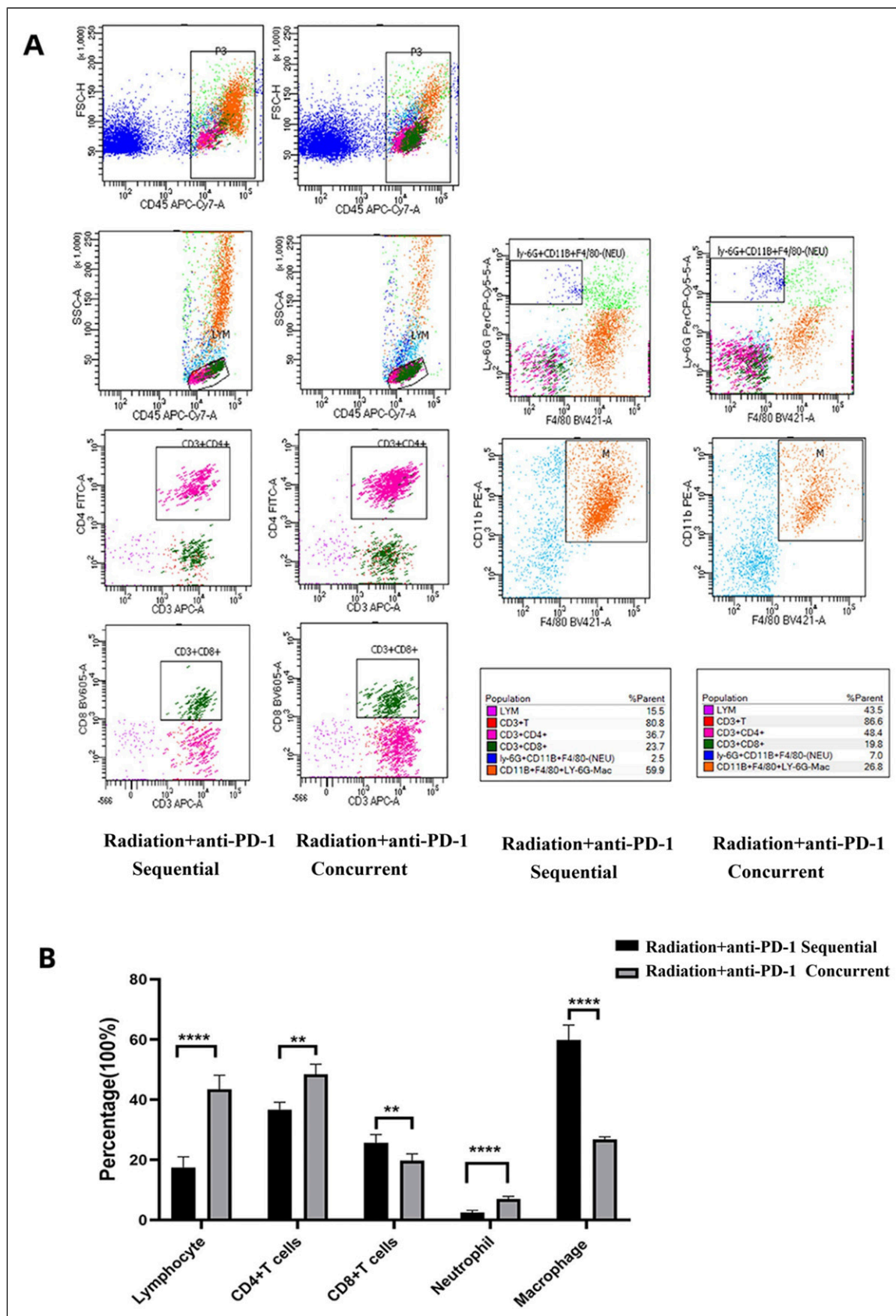


**Figure 3.** Proportion of inflammatory cells in BALF. Representative images of the proportion of inflammatory cells in BALF across different groups are shown. (B) Statistical analysis of the proportion of inflammatory cells in BALF in different groups. \* $P < .05$ , \*\* $P < .01$ , \*\*\* $P < .001$ , \*\*\*\* $P < .0001$ , NS, not significant.

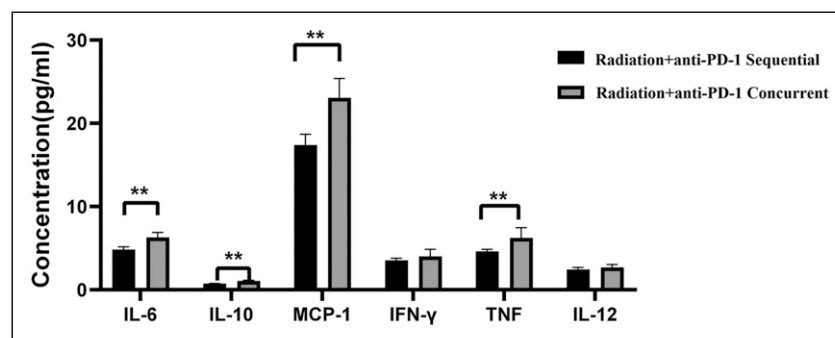


**Figure 4.** Statistical analysis of inflammatory cytokines in BALF in different groups. \* $P < .05$ , \*\* $P < .01$ .

LUN 14-179 study utilized pembrolizumab for maintenance treatment, aligning with the methodology of the PACIFIC study.<sup>22</sup>

It had been reported that the first approach of combination therapy might result in more pronounced adverse reactions. According to a study analyzing 1113 patients with NSCLC across 11 clinical trials, the concurrent treatment approach had been associated with a higher prevalence of severe adverse events (AEs) (41.6% vs 24.8%) and pneumonitis (7.1% vs 3.9%) compared to the sequential treatment approach.<sup>23</sup> Until now, the pathophysiological alterations resulting from concurrent or sequential approach had not yet to be reported.

As evidenced by morphological examination, our study found that lung injury was more severe in the concurrent treatment group compared to the sequential treatment group. BALF and lung tissue were collected and analyzed, revealing an increase in inflammatory cytokines and infiltration of inflammatory cells in the group receiving concurrent treatment.

Our study observed a significant increase in neutrophils and lymphocytes in BALF in the concurrent treatment group compared to the sequential treatment group. Additionally, there was a notable elevation in the levels of neutrophils, lymphocytes, and macrophages in lung tissue sections. Neutrophils and lymphocytes in BALF were pivotal cellular components involved in the response to pulmonary inflammation.<sup>24,25</sup> Previous studies had documented a significant increase in lymphocytes and neutrophils in BALF in cases of ICIs-associated pneumonitis,<sup>24</sup> with elevated ratios of these cells observed in symptomatic radiation pneumonitis compared to asymptomatic cases.<sup>25</sup> In lung tissue sections, alongside the observed increase in neutrophils and lymphocytes in BALF, we also noted an enhanced infiltration of macrophages. Macrophages were critical immune cells that play essential roles in maintaining tissue homeostasis and mediating inflammatory responses.<sup>26</sup> In the analysis of BALF, the concurrent treatment group did not exhibit an increase in macrophage numbers. We interpreted this finding to suggest that in the CD45-positive cell population of the BALF, there was a more pronounced increase in the numbers of neutrophils and lymphocytes compared to macrophages. Consequently,

this resulted in a reduced proportion of macrophages relative to the total immune cell population.

Additionally, our findings indicated a significant elevation in the levels of IL-6, MCP-1, and TNF in the BALF of the concurrent treatment group. IL-6 was a circulating cytokine secreted by various cell types, including activated macrophages and lymphocytes,<sup>27</sup> and played a crucial role in the inflammatory response to infection and injury,<sup>28</sup> subsequently recruiting inflammatory cells to the endothelium.<sup>29</sup> MCP-1, also secreted by inflammatory cells, had been demonstrated to facilitate the migration of monocytes to sites of inflammation<sup>30</sup> and was upregulated during acute inflammatory processes.<sup>31</sup> TNF was an inflammatory cytokine primarily produced by macrophages and monocytes,<sup>32</sup> and its excessive production played a crucial role in the induction of inflammatory genes, promotion of cell death, upregulation of endothelial cells, and the recruitment and activation of immune cells.<sup>33,34</sup> We hypothesized that the increased levels of these cytokines in BALF lead to the infiltration of neutrophils, lymphocytes, and macrophages into the lung tissue. The activation of these infiltrating inflammatory cells was likely to sustain the release of inflammatory cytokines, thereby aggravating lung tissue injury.

Building on prior research, we supposed that crosstalk between signaling pathways involved in radiation-induced lung injury and immune-mediated lung injury, which may exacerbate the recruitment of inflammatory cells and the production of cytokines during concurrent treatment. First, both radiation and ICIs could stimulate damage-associated signaling pathways, including the ROS/reactive nitrogen species (RNS) and Cyclic Guanosine Monophosphate-Adenosine Monophosphate (cGMP-AMP) synthase-stimulator of interferon genes (cGAS-STING) signaling pathways, which participated in the initial process of lung injury.<sup>35,36</sup> Second, TGF- $\beta$  was elevated in both ICIs-associated pneumonitis and radiation pneumonitis, so TGF- $\beta$  might be a key molecule in the crosstalk of signaling pathways.<sup>37,38</sup>

Our research possessed certain clinical significance. For patients at elevated risk for pneumonitis, such as those who were elderly or had a history of chronic obstructive pulmonary

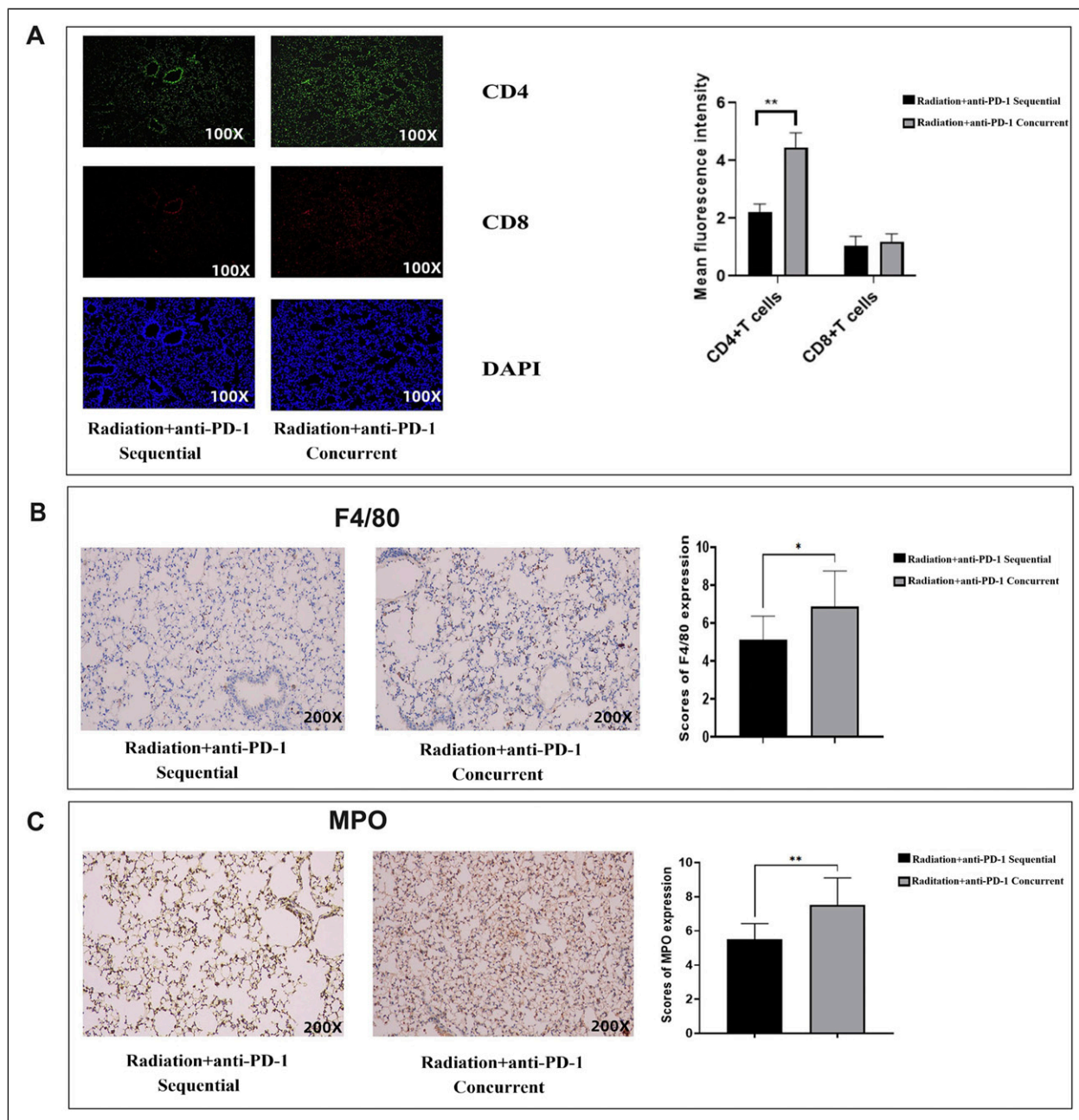


**Figure 5.** Recruitment of inflammatory infiltration cells in the lung tissue. (A) T lymphocytes infiltrated lung tissue in different groups. Green fluorescence: CD4<sup>+</sup>T cells, red fluorescence: CD8<sup>+</sup>T cells, and DAPI: blue fluorescence. (B) Infiltrating macrophages in lung tissue in different groups. (C) Infiltrating neutrophils in lung tissue in different groups. \* $P < .05$ , \*\* $P < .01$ .

disease (COPD), the sequential administration of ICIs might potentially alleviate the acute inflammatory effects on the lungs, thereby improving the safety profile of combination therapy. Based on prior animal models, the 4-week period following exposure to chest X-rays was considered an ‘immediate phase.’<sup>39</sup> Avoiding administration during this period might constitute a safer strategy.

Nonetheless, our study had several limitations. First, the impact of the administration sequence following thoracic

radiation on anti-tumor efficacy remains ambiguous. Determining whether concurrent or sequential administration was more effective for tumor control requires additional clinical data. Despite the existence of Phase III PACIFIC-2 studies, the concurrent administration of chemoradiotherapy and durvalumab failed to achieve the primary study endpoint.<sup>40</sup> This outcome contrasted with the findings of the PACIFIC study,<sup>21</sup> which demonstrated that sequential treatment involving chemoradiotherapy followed by durvalumab can extend

progression-free survival (PFS). Second, regarding sequential therapy, the optimal timing for administration post-radiation was uncertain. The animal model indicated an immediate phase of 4 weeks, whereas another retrospective study identified 14 days as the threshold distinguishing sequential from concurrent treatment.<sup>11</sup> Lastly, our research was conducted on a limited sample of mice, and the applicability of these findings to humans needed validation through clinical studies.

## Conclusion

This study provided a novel perspective on the optimal integration of radiotherapy and PD-1, underscoring the necessity for further research into the underlying mechanisms and phenomena associated with their combined application.

## Acknowledgments

We acknowledged Dr Xianchao Zhang for his kind help in pathological analysis.

## Author Contributions

Peng Yan: Visualization, Writing-original draft and Funding acquisition. Zewen Wang: Prepared IHC, IF and photographed. Yufeng Wang: Experiments on animals and Flow cytometry. Yongliang Liu: Experiments on animals and Radiation preparation. Anna Tong: Methodology and Data curation. Meili Sun: Methodology, Writing-review, Editing and Supervision.

## Declaration of Conflicting Interests

The author(s) declared no potential conflicts of interest with respect to the research, authorship, and/or publication of this article.

## Funding

The author(s) disclosed receipt of the following financial support for the research, authorship, and/or publication of this article: Youth Project of Natural Science Foundation of Shandong Province (ZR2022QH187); Shandong Province Traditional Chinese Medicine Science and Technology Project (Q-2022004).

## ORCID iD

Peng Yan  <https://orcid.org/0000-0002-4256-6323>

## References

1. Vinod SK, Hau E. Radiotherapy treatment for lung cancer: current status and future directions. *Respirology*. 2020;25(Suppl 2):61-71.
2. Brown S, Banfill K, Aznar MC, Whitehurst P, Faivre Finn C. The evolving role of radiotherapy in non-small cell lung cancer. *Br J Radiol*. 2019;92:20190524.
3. Yang WC, Hsu FM, Yang PC. Precision radiotherapy for non-small cell lung cancer. *J Biomed Sci*. 2020;27:82.
4. Boustani J, Créhange G. Dose-escalated radiotherapy in esophageal cancer: a review of the literature. *Cancer Radiother*. 2022;26:884-889.
5. Hsieh K, Dickstein DR, Runnels J, et al. Radiotherapy and immunotherapy in lung cancer. *Biomedicines*. 2023;11:1642.
6. Yang H, Jin T, Li M, Xue J, Lu B. Synergistic effect of immunotherapy and radiotherapy in non-small cell lung cancer: current clinical trials and prospective challenges. *Precis Clin Med*. 2019;2:57-70.
7. Keffer S, Guy CL, Weiss E. Fatal radiation pneumonitis: literature review and case series. *Adv Radiat Oncol*. 2020;5:238-249.
8. Naidoo J, Wang X, Woo KM, et al. Pneumonitis in patients treated with anti-programmed death-1/programmed death ligand 1 therapy. *J Clin Oncol*. 2017;35:709-717.
9. Shaverdian N, Lisberg AE, Bornazyan K, et al. Previous radiotherapy and the clinical activity and toxicity of pembrolizumab in the treatment of non-small-cell lung cancer: a secondary analysis of the KEYNOTE-001 phase 1 trial. *Lancet Oncol*. 2017;18:895-903.
10. Theelen W, Peulen H, Lalezari F, et al. Effect of pembrolizumab after stereotactic body radiotherapy vs pembrolizumab alone on tumor response in patients with advanced non-small cell lung cancer: results of the PEMBRO-RT phase 2 randomized clinical trial. *JAMA Oncol*. 2019;5:1276-1282.
11. Bang A, Wilhite TJ, Pike L, et al. Multicenter evaluation of the tolerability of combined treatment with PD-1 and CTLA-4 immune checkpoint inhibitors and palliative radiation therapy. *Int J Radiat Oncol Biol Phys*. 2017;98:344-351.
12. Zhang NZX, Kong CSX, Chen CJN, et al. Application of anti-PD1 drugs before or during thoracic radiotherapy increases the incidence of radiation pneumonia compared to the application after radiotherapy. *Ann Oncol*. 2020;31:S1081.
13. Gao J, Peng S, Shan X, et al. Inhibition of AIM2 inflammasome-mediated pyroptosis by andrographolide contributes to amelioration of radiation-induced lung inflammation and fibrosis. *Cell Death Dis*. 2019;10:957.
14. Peters S, Reck M, Smit EF, Mok T, Hellmann MD. How to make the best use of immunotherapy as first-line treatment of advanced/metastatic non-small-cell lung cancer. *Ann Oncol*. 2019;30:884-896.
15. Wang F, Luo Y, Tian X, et al. Impact of radiotherapy concurrent with anti-PD-1 therapy on the lung tissue of tumor-bearing mice. *Radiat Res*. 2019;191:271-277.
16. Mikawa K, Nishina K, Takao Y, Obara H. ONO-1714, a nitric oxide synthase inhibitor, attenuates endotoxin-induced acute lung injury in rabbits. *Anesth Analg*. 2003;97:1751-1755.
17. Aboushousha T, Mamdouh S, Hamdy H, et al. Immunohistochemical and biochemical expression patterns of TTF-1, RAGE, GLUT-1 and SOX2 in HCV-associated hepatocellular carcinomas. *Asian Pac J Cancer Prev APJCP*. 2018;19:219-227.
18. Liu M, Liu Q, Pei Y, et al. Aqp-1 gene knockout attenuates hypoxic pulmonary hypertension of mice. *Arterioscler Thromb Vasc Biol*. 2019;39:48-62.



19. Peters S, Felip E, Dafni U, et al. Safety evaluation of nivolumab added concurrently to radiotherapy in a standard first line chemoradiotherapy regimen in stage III non-small cell lung cancer-The ETOP NICOLAS trial. *Lung Cancer*. 2019;133:83-87.
20. Jabbour SK, Lee KH, Frost N, et al. Pembrolizumab plus concurrent chemoradiation therapy in patients with unresectable, locally advanced, stage III non-small cell lung cancer: the phase 2 KEYNOTE-799 nonrandomized trial. *JAMA Oncol*. 2021;7:1-9.
21. Antonia SJ, Villegas A, Daniel D, et al. Overall survival with durvalumab after chemoradiotherapy in stage III NSCLC. *N Engl J Med*. 2018;379:2342-2350.
22. Durm GA, Jabbour SK, Althouse SK, et al. A phase 2 trial of consolidation pembrolizumab following concurrent chemoradiation for patients with unresectable stage III non-small cell lung cancer: hoosier cancer research network LUN 14-179. *Cancer*. 2020;126:4353-4361.
23. Li B, Jiang C, Pang L, et al. Toxicity profile of combining PD-1/PD-L1 inhibitors and thoracic radiotherapy in non-small cell lung cancer: a systematic review. *Front Immunol*. 2021;12:627197.
24. Nishiyama O, Shimizu S, Haratani K, et al. Clinical implications of bronchoscopy for immune checkpoint inhibitor-related pneumonitis in patients with non-small cell lung cancer. *BMC Pulm Med*. 2021;21:155.
25. Toma CL, Serbescu A, Alexe M, Cervis L, Ionita D, Bogdan MA. The bronchoalveolar lavage pattern in radiation pneumonitis secondary to radiotherapy for breast cancer. *Maedica (Bucur)*. 2010;5:250-257.
26. Watanabe S, Alexander M, Misharin AV, Budinger GRS. The role of macrophages in the resolution of inflammation. *J Clin Invest*. 2019;129:2619-2628.
27. Wu W, Li Z, Tang T, Wu J, Liu F, Gu L. 5-HTR2A and IL-6 polymorphisms and obstructive sleep apnea-hypopnea syndrome. *Biomed Rep*. 2016;4:203-208.
28. Aroor AR, McKarns S, Demarco VG, Jia G, Sowers JR. Maladaptive immune and inflammatory pathways lead to cardiovascular insulin resistance. *Metabolism*. 2013;62:1543-1552.
29. Shapouri-Moghaddam A, Mohammadian S, Vazini H, et al. Macrophage plasticity, polarization, and function in health and disease. *J Cell Physiol*. 2018;233:6425-6440.
30. Jiang Y, Beller DI, Frenzl G, Graves DT. Monocyte chemoattractant protein-1 regulates adhesion molecule expression and cytokine production in human monocytes. *J Immunol*. 1992;148:2423-2428.
31. Kaliora AC, Stathopoulou MG, Triantafyllidis JK, Dedoussis GV, Andrikopoulos NK. Alterations in the function of circulating mononuclear cells derived from patients with Crohn's disease treated with mastic. *World J Gastroenterol*. 2007;13:6031-6036.
32. Marzoq AJ, Mustafa SA, Heidrich L, Hoheisel JD, Alhamdani MSS. Impact of the secretome of activated pancreatic stellate cells on growth and differentiation of pancreatic tumour cells. *Sci Rep*. 2019;9:5303.
33. Shen HM, Pervaiz S. TNF receptor superfamily-induced cell death: redox-dependent execution. *FASEB J*. 2006;20:1589-1598.
34. Warren JS, Ward PA, Johnson KJ. Tumor necrosis factor: a plurifunctional mediator of acute inflammation. *Mod Pathol*. 1988;1:242-247.
35. Chen Q, Sun L, Chen ZJ. Regulation and function of the cGAS-STING pathway of cytosolic DNA sensing. *Nat Immunol*. 2016;17:1142-1149.
36. Wan D, Jiang W, Hao J. Research advances in how the cGAS-STING pathway controls the cellular inflammatory response. *Front Immunol*. 2020;11:615.
37. Derynck R, Turley SJ, Akhurst RJ. TGF $\beta$  biology in cancer progression and immunotherapy. *Nat Rev Clin Oncol*. 2021;18:9-34.
38. Zhang Z, Zhou J, Verma V, et al. Crossed pathways for radiation-induced and immunotherapy-related lung injury. *Front Immunol*. 2021;12:774807.
39. Ghita M, Dunne V, Hanna GG, Prise KM, Williams JP, Butterworth KT. Preclinical models of radiation-induced lung damage: challenges and opportunities for small animal radiotherapy. *Br J Radiol*. 2019;92:20180473.
40. Bradley JD, Sugawara S, Lee KHH, et al. Durvalumab in combination with chemoradiotherapy for patients with unresectable stage III NSCLC: final results from PACIFIC-2. *Ann Oncol*. 2024;9(suppl\_3):1-12.